High-resolution, background-free, time-to-space conversion by collinearly phase-matched sum-frequency generation

Dror Shayovitz and Dan M. Marom*

Department of Applied Physics, Hebrew University of Jerusalem, Jerusalem 91904, Israel
**Corresponding author: danmarom@cc.huji.ac.il*

Received March 17, 2011; revised April 20, 2011; accepted April 22, 2011;
posted April 22, 2011 (Doc. ID 144400); published May 20, 2011

We report the first demonstration, to our knowledge, of time-to-space conversion of 1.55 μm femtosecond optical pulses using nondegenerate, collinearly phase-matched sum-frequency generation. A quasi-monochromatic and background-free output signal spanning a time window of 35 ps and with a pulse image width of 350 fs was achieved. The resulting serial-to-parallel resolution factor of 100 demonstrates the potential for all-optical complete frame demultiplexing of a 1 Tbit/s optical time-division multiplexing bit stream. © 2011 Optical Society of America

OCIS codes: 320.7085, 190.4223, 060.4230.

The use of optical time-division multiplexing (OTDM) in high-speed optical communications is a possible solution to the challenge of supporting ever-increasing capacity requirements while avoiding the overhead costs associated with high channel-count wavelength-division multiplexed systems. A recent demonstration of 5.1 Tbit/s data transmission achieved at 1.28 Tbaud/s signaling with phase-shift keying (PSK) [1] demonstrates the bandwidth efficiency potential of coherent detection OTDM. However, signal recovery at Tbit/s bit rates poses a serious challenge, because available optoelectronic receivers are limited to electrical bandwidths of 50–100 GHz. A solution that has attracted much attention is all-optical demultiplexing using fast optical nonlinearities.

Time-to-space conversion [2–8] is a real-time optical demultiplexing technique that utilizes sum-frequency generation (SFG) between a frame of signal pulses and a reference pulse to convert a fast serial OTDM pulse stream to a number of slower spatially parallel channels, which can then be directly detected by an array of optoelectronic receivers. Key advantages of this technique are the strong $\chi^{(2)}$ nonlinearity of certain nonlinear crystals and the preservation of phase information for compatibility with advanced modulation formats such as PSK. Time-to-space conversion has been demonstrated in the optical communications band [8], but with relatively low conversion efficiency. A limiting factor on the conversion efficiency is the short interaction length of two crossed beams in noncollinear phase-matching, which is required to provide a background-free output signal. One way to improve the conversion efficiency is to use birefringent phase-matching with copropagating beams, thus increasing the interaction length up to the focused beams' confocal length. However, in the collinear configuration, the information-bearing SFG signal is superimposed over the second harmonic generation (SHG) background light from the signal and reference pulses independently and will coherently interfere with it.

In this Letter, we report the first (to our knowledge) demonstration of time-to-space conversion by means of collinear nondegenerate wave mixing with a background-free output image. By employing nondegenerate wavelength mixing, the SFG product is generated at a different wavelength from the two SHG background components. Spectral filtering of the generated light then provides a background-free output signal. Detailed analyses of the operation of a time-to-space conversion processor are provided in [2,3,7] and briefly summarized here. A sequence of input signal pulses (a "frame") and the locally generated reference pulse both enter the processor. Each of these waveforms is then spatially dispersed in opposite directions with a grating and lens combination, so that the high-frequency components of the signal waveform spatially overlap the low-frequency components of the reference pulse, and vice versa. A nonlinear crystal is located at the Fourier plane where the dispersed light is spatially resolved. SFG between the spectral components at every spatial location results in a quasi-monochromatic upconverted wave. This generated wave contains a linear phase tilt across the beam that is proportional to the time delay between each signal pulse in the frame and the reference pulse. A spatial Fourier transform by an output lens converts this phase tilt to a spatial translation at the image plane, resulting in a

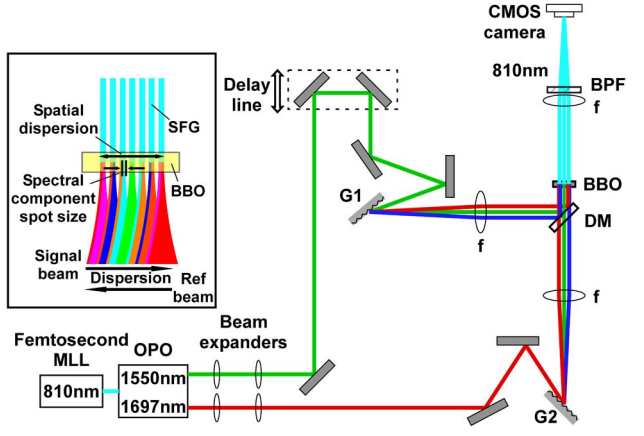

Fig. 1. (Color online) Experimental setup (MLL, mode-locked laser; OPO, optical parametric oscillator; G1/G2, grating; f, Fourier lens; DM, dichroic mirror; BBO, beta barium borate nonlinear crystal; BPF, bandpass filter. Inset: collinear, oppositely dispersed signal and reference beams at the nonlinear crystal.

Table 1. Input Beam Characteristics of Time-to-Space Converter[a]

	λ_0(nm)	f_g (lp/mm)	α (°)	$dx/d\omega$ (μm/GHz)	w_0 (μm)	P_{av}/P_{max}(mW/kW)
Signal	1550	1100	70.0	−0.16	13	215/27
Ref.	1697	1000	79.8	0.16	14	85/11

[a] λ_0, central wavelength; f_g, grating frequency; α, angle of incidence on grating; $dx/d\omega$, spatial dispersion; w_0, focused spot radius of single spectral component; P_{av}/P_{max}, average beam power/peak power at crystal. Ideally the reference beam power would be higher than the signal power.

transverse spatial pattern that is the direct image of the input signal waveform.

Figure 1 shows our experimental setup. The signal (at 1550 nm) and idler (at 1697 nm) outputs of a Spectra-Physics Opal (Newport Corporation, USA) optical parametric oscillator (with FWHM pulse duration of 100 fs and repetition rate of 80.2 MHz) are expanded to appropriate collimated beam sizes and undergo equal but opposite linear spatial dispersions by diffraction gratings G1 and G2 and 75 mm Fourier lenses. The two dispersed beams are superimposed by a long-pass dichroic mirror (DM) and are incident on a 1 mm-thick beta barium borate (BBO) nonlinear crystal located at the focal plane. The confocal length of the focused signal and reference beams in the plane of dispersion was calculated as 1.1 mm (per spectral component). The relevant beam characteristics are listed in Table 1.

Because of the matched yet flipped spatial dispersions of the signal and reference beams at the BBO crystal, Type I phase-matched SFG at each point in space results in a quasi-monochromatic output beam at 810 nm. An output lens of focal length 75 mm coherently focuses the light to a narrow line at the Fourier plane, where a CMOS camera records the output spatial image. The SFG −3 dB bandwidth was measured as 0.22 nm (= 100 GHz) centered at 810 nm by coupling focused output light into a multimode fiber connected to an optical spectrum analyzer (Fig. 2). This narrow signal bandwidth demonstrates compatibility with optoelectronic receivers and also the possibility of mixing the SFG signal with a CW local oscillator at the same wavelength to extract phase information. Background second harmonic light at 775 nm and 849 nm is blocked by a bandpass filter (central wavelength 810 nm, −3 dB bandwidth 10 nm) placed between the lens and the camera.

The key performance parameters of the time-to-space converter are the serial-to-parallel resolution factor N and the conversion efficiency η. The serial-to-parallel resolution factor N is defined as the ratio of the time window, ΔT (which limits the maximum extent of the output spatial pattern), to the width of an individual pulse image, τ, and determines the maximum number of pulses that can be simultaneously demultiplexed to separate spatial channels. The conversion efficiency η is defined as the SFG output power divided by the signal beam power incident on the nonlinear crystal. The resolution–conversion efficiency product is invariant to the spot size, w_0, of a spectral component focused at the crystal, so that one can be improved at the expense of the other. However, N is dictated by the application and, for demultiplexing a 1 Tbit/s OTDM signal down to electrical bandwidths, should be between 40 and 100.

The time-to-space conversion factor and the time window were measured by varying the time delay between the signal and reference pulses (Fig. 3). A linear fit to the time-delay-dependent pulse image position data results in a time-to-space conversion factor of 60 μm/ps. A Gaussian curve was fitted to the time-delay-dependent pulse image intensity data giving a FWHM time window of 35 ps. The conversion efficiency was calculated by measuring the SFG output power with a power meter placed after the bandpass filter and dividing by the signal beam power incident on the BBO crystal at zero time delay (peak efficiency). The linear conversion efficiency slope was measured as 11.2×10^{-5} per watt of reference beam power and the maximum conversion efficiency obtained was 0.9×10^{-5} at 85 mW reference beam power. This low conversion efficiency is primarily due to the low reference beam power available in our setup and is also due to the spatial walkoff (48.9 mrad) limited interaction length in the BBO crystal. Note that the spatial walkoff limitation can be overcome by using noncritical phase-matching [3] or quasi-phase-matching [8]. Because we are operating in the linear conversion regime (i.e., with nondepleting pump power), we would benefit from

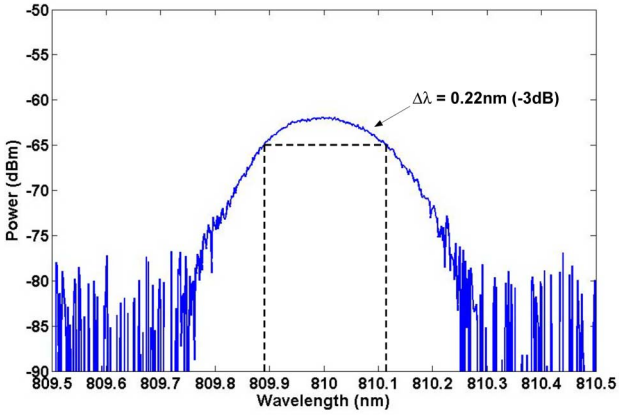

Fig. 2. (Color online) SFG narrowband spectrum centered at 810 nm with a −3 dB bandwidth of 0.22 nm (= 100 GHz).

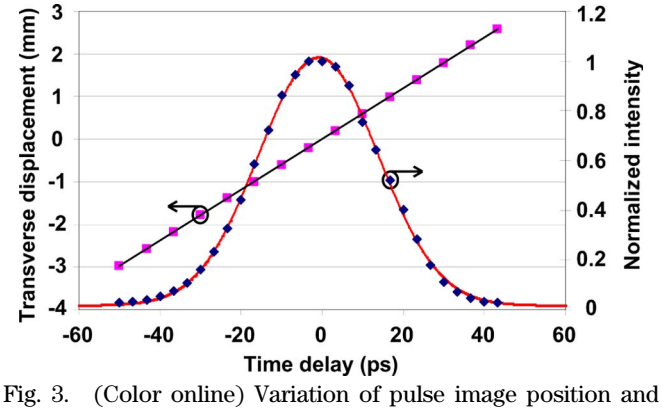

Fig. 3. (Color online) Variation of pulse image position and intensity as a function of time delay, showing linear and Gaussian fits, respectively.

Table 2. Calculated and Measured Time-to-Space Conversion Parameters[a]

	$\Delta x/\Delta t$ (μm/ps)	ΔT (ps)	τ (ps)	N	η (%)
Predicted	57	34	0.15	227	1.7×10^{-3}
Measured	60	35	0.35	100	0.9×10^{-3}

[a] $\Delta x/\Delta t$, time-to-space conversion factor; ΔT, FWHM time window; τ, FWHM pulse image width; N, serial-to-parallel resolution factor; η, conversion efficiency.

a more intense reference pulse. The results are summarized and compared with the theoretically calculated parameters in Table 2.

The time-to-space converted pulse image width τ was estimated by fitting a Lorentzian curve to a pulse image at the center of the time window, with the resulting FWHM corresponding to 350 fs. Note that because the signal and reference pulses are of the same duration, an autocorrelation factor of 1.5 has been included in the values of the theoretical time window and pulse image width. It can be seen that the measured pulse image width is more than twice as long as the predicted value. We attribute this loss of resolution to a narrowing of the phase-matched bandwidth due to distortions in the dispersed reference beam spectrum, which result from the asymmetric spatial profile of the reference beam incident on the diffraction grating. This reduction in the SFG interaction bandwidth results in a less spectrally resolved SFG output beam and therefore a less tightly focused pulse image.

Despite this, the high time-to-space conversion resolution of $N = 100$ demonstrates the potential for 1-to-50 demultiplexing of subpicosecond pulses with low interchannel cross talk. As a demonstration, a series of 35 pulse images equally spaced throughout the 35 ps time window (equivalent to 1 THz OTDM baud rate) was recorded [Figs. 4(a) and 4(b)]. In addition to the time-delay-dependent intensity of the output image, it is noted that there is a defocusing effect toward one side of the time window [the right-hand side in Figs. 4(a) and 4(b)]. We attribute this again to an asymmetry in the spectral profile of the dispersed reference beam. This spectral asymmetry results in a more limited range of phase-matched signal and reference frequency components toward one side of the time window, giving a less tightly focused output image. It may be possible to correct this distortion by spatially filtering the reference beam before it reaches the diffraction grating, at the expense of reference beam power.

The important innovation of our work is the implementation of background-free, high-resolution time-to-space conversion using nondegenerate, collinearly phase-matched SFG. This opens the way to a further advance by employing quasi-phase-matching in a periodically poled lithium niobate crystal, thus overcoming the spatial walkoff limitation on the interaction length and increasing the conversion efficiency.

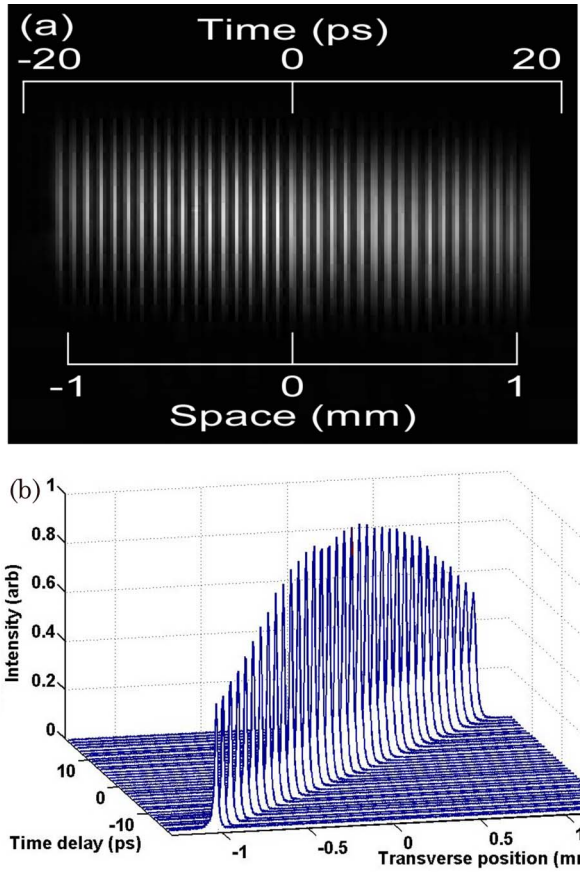

Fig. 4. (Color online) (a) 35 pulse spatial images representing a synthetic 1 Tbit/s data stream (composite image) and (b) variation in pulse image intensity and transverse position as the time delay is varied throughout the time window.

The authors gratefully acknowledge the support of The Peter Brodje Center for Innovative Engineering.

References

1. H. C. H. Mulvad, M. Galili, L. Oxenlowe, H. Hu, A. T. Clausen, J. B. Jensen, C. Peucheret, and P. Jeppesen, Opt. Express **18**, 1438 (2010).
2. P.-C. Sun, Y. T. Mazurenko, and Y. Fainman, J. Opt. Soc. Am. A **14**, 1159 (1997).
3. A. M. Kan'an and A. M. Weiner, J. Opt. Soc. Am. B **15**, 1242 (1998).
4. K. Oba, P.-C. Sun, Y. T. Mazurenko, and Y. Fainman, Appl. Opt. **38**, 3810 (1999).
5. J. Ishi, H. Kunugita, T. Ban, T. Kondo, and K. Ema, Appl. Phys. Lett. **77**, 3487 (2000).
6. D. M. Marom, D. Panasenko, P.-C. Sun, and Y. Fainman, IEEE J. Sel. Top. Quantum Electron. **7**, 683 (2001).
7. D. M. Marom, D. Panasenko, P.-C. Sun, Y. T. Mazurenko, and Y. Fainman, J. Opt. Soc. Am. A **18**, 448 (2001).
8. J.-H. Chung and A. M. Weiner, J. Lightwave Technol. **21**, 3323 (2003).